CHEMMEDCHEM
Chemistry & Drug Discovery

Supporting Information

The Predicted Ensemble of Low-Energy Conformations of Human Somatostatin Receptor Subtype 5 and the Binding of Antagonists

Sijia S. Dong,[a] Ravinder Abrol,[a, b] and William A. Goddard, III*[a]

cmdc_201500023_sm_miscellaneous_information.pdf

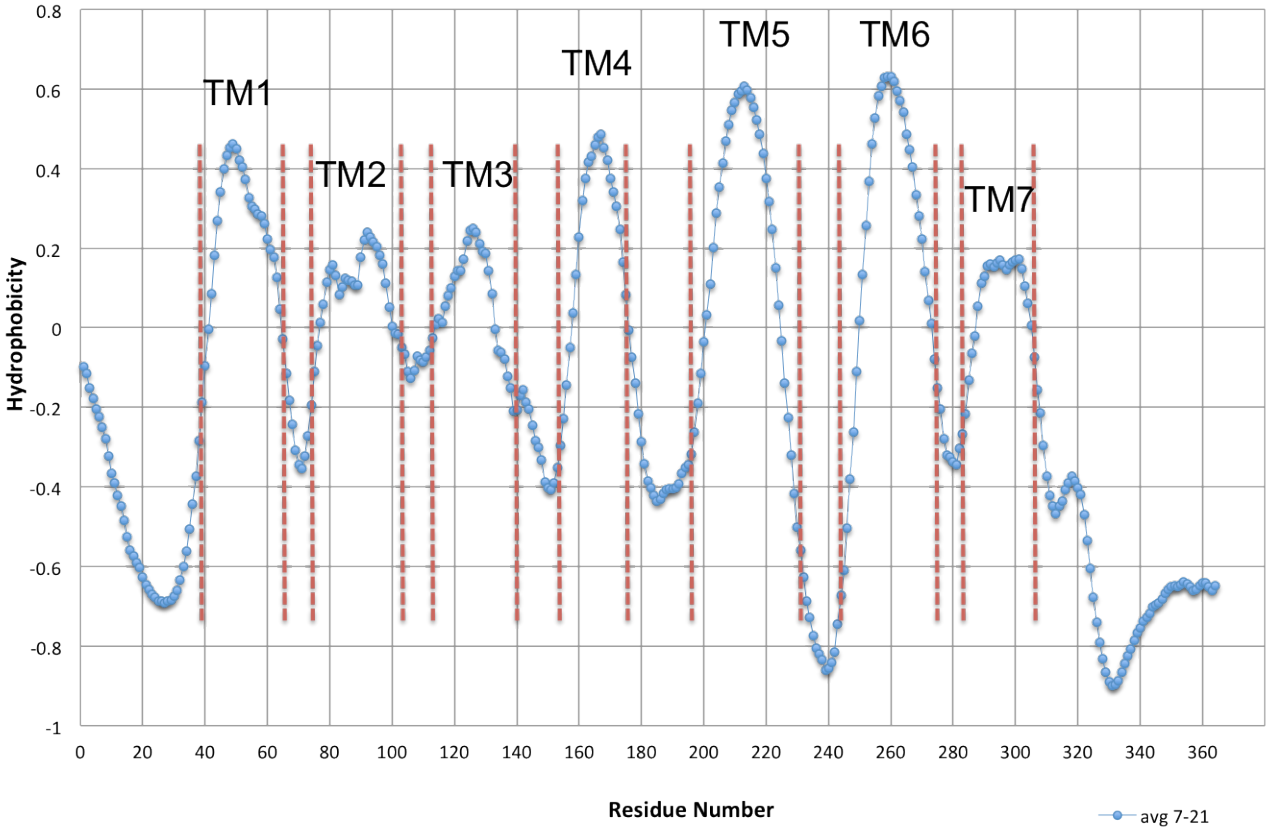

Figure S1. Hydrophobicity profile of hSSTR5 before applying the capping rules. The residues expected to lie in the membrane are indicated by red dashed lines.

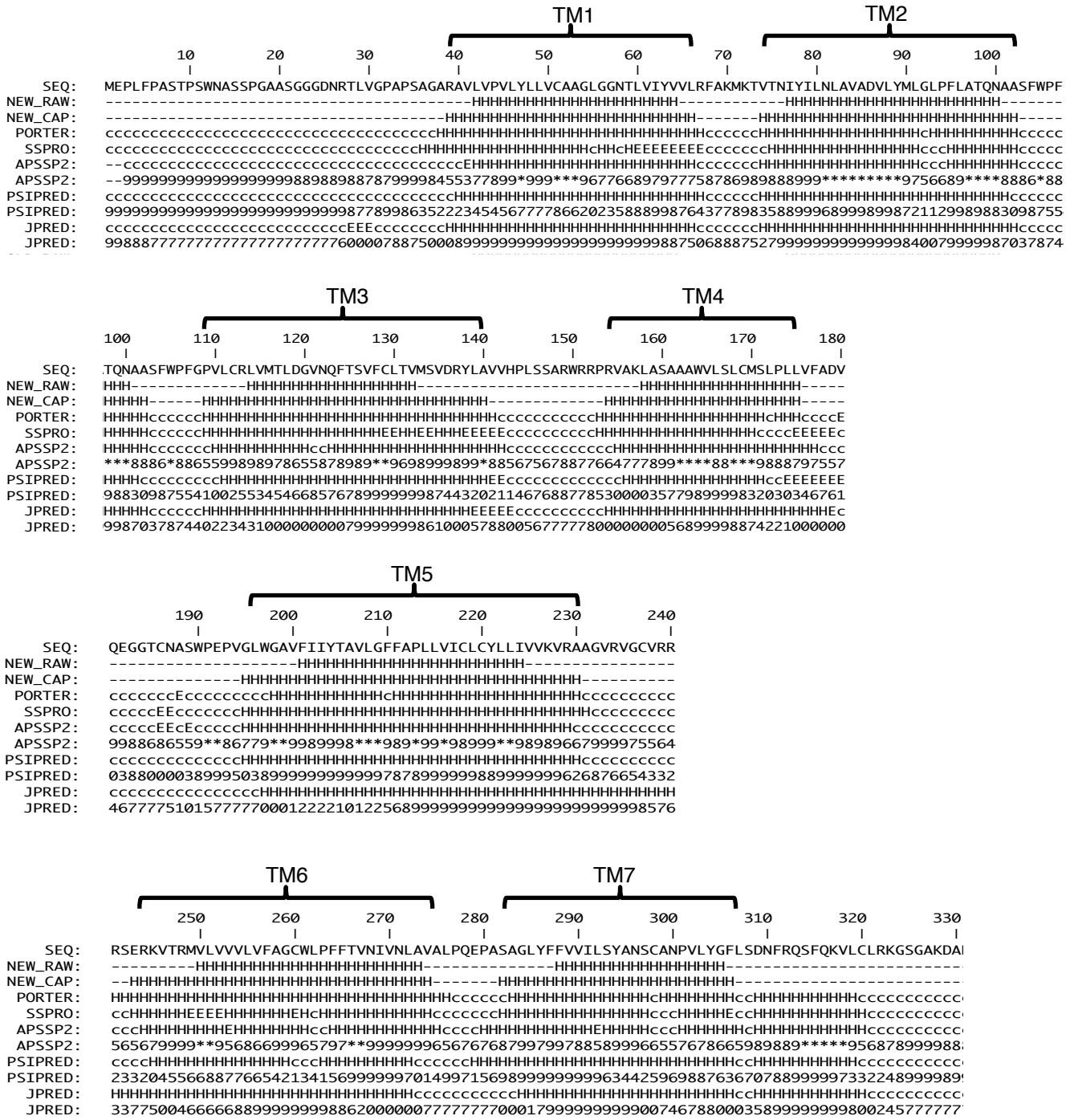

Figure S2. Secondary structure prediction for hSSTR5 from various servers. NEW_RAW is PredicTM prediction; NEW_CAP is from consensus of different secondary structure prediction servers.

Table S1. Sequence similarity (in percentage) between hSSTR5 and Class A GPCRs with experimentally available structures. The bold underlined cases were used as templates in this study.

Protein Identifier	Rank	All	TM Avg	TM1	TM2	TM3	TM4	TM5	TM6	TM7
P35346|SSR5_HUMAN	1	100.00	100.00	100.00	100.00	100.00	100.00	100.00	100.00	100.00
P41146|OPRX_HUMAN	**24**	**33.79**	**46.79**	**56.52**	**58.33**	**47.37**	**22.22**	**41.67**	**45.83**	**55.56**
P42866|OPRM_MOUSE	**29**	**33.24**	**44.62**	**52.17**	**50.00**	**42.11**	**27.78**	**33.33**	**45.83**	**61.11**
P32300|OPRD_MOUSE	37	34.07	43.96	47.83	50.00	47.37	27.78	33.33	45.83	55.56
P41145|OPRK_HUMAN	**42**	**31.04**	**40.33**	**39.13**	**50.00**	**47.37**	**16.67**	**33.33**	**45.83**	**50.00**
P61073|CXCR4_HUMAN	83	23.63	32.13	39.13	45.83	31.58	16.67	33.33	25.00	33.33
P02699|OPSD_BOVIN	432	20.05	29.99	26.09	33.33	15.79	33.33	45.83	33.33	22.22
P07700|ADRB1_MELGA	464	20.33	33.73	34.78	25.00	26.32	16.67	29.17	54.17	50.00
P07550|ADRB2_HUMAN	574	18.68	27.59	30.43	25.00	21.05	16.67	20.83	45.83	33.33
P31356|OPSD_TODPA	764	17.03	26.44	30.43	29.17	15.79	11.11	45.83	25.00	27.78
P08172|ACM2_HUMAN	1027	19.23	30.37	17.39	25.00	36.84	44.44	25.00	25.00	38.89
P29274|AA2AR_HUMAN	1042	16.76	27.74	21.74	20.83	21.05	33.33	25.00	33.33	38.89
P08483|ACM3_RAT	1231	18.13	30.62	26.09	29.17	36.84	27.78	25.00	25.00	44.44

Table S2. Top 10 structures from the BiHelix/CombiHelix predictions for all 15 starting structures. [a] The lowest energy case for each template (shaded) was used for the SuperBiHelix step. [b] The Δη values are the deviations of helix (H) rotation angles from the respective homology templates.

Method	Δη[b] [°]							Energy [kcal mol^{-1}]				
	H1	H2	H3	H4	H5	H6	H7	CInterH	CTotal	NInterH	NTotal	E_{CNti}
mOPRM homology[a]	0	0	0	0	0	0	0	-418.5	-225.2	-386.9	-349.4	-345.0
mOPRM homology	0	0	0	0	120	0	0	-378.1	-181.0	-351.0	-299.4	-302.4
mOPRM homology	0	0	0	0	90	0	0	-380.5	-158.8	-359.9	-305.7	-301.2

mOPRM homology	0	0	0	-30	0	0	0	-390.2	-145.8	-359.7	-305.8	-300.4
mOPRM homology	0	0	0	0	-30	0	0	-396.4	-131.5	-369.8	-274.3	-293.0
hOPRK homology	0	0	0	0	30	0	0	-407.0	-112.4	-372.6	-255.7	-286.9
mOPRM homology	0	0	0	0	-120	90	-30	-370.4	-123.3	-354.6	-290.8	-284.8
hOPRX homology	0	0	0	0	0	0	0	-381.2	-124.0	-363.4	-257.1	-281.4
mOPRM homology	0	0	0	-30	30	0	0	-382.2	-129.4	-353.8	-254.0	-279.9
mOPRM homology	0	0	0	0	-150	90	-30	-353.2	-133.7	-337.6	-290.2	-278.7

Table S3. Sampling space of the coarse SuperBiHelix for each of the three templates. The deviation angles apply to every helix (H) unless otherwise labeled. The angles apply specifically to one helix are from top 20 BiHelix results of the respective template. The starting structure of the sampling is the lowest energy case in BiHelix for each template (the shaded cases in Table S2).

Template	Δθ [°]	Δφ [°]	Δη [°]
mOPRM	0, ±15	0, ±45, ±90	0, ±30, -60 (H6), -90 (H5, H6), -120 (H5), -150 (H5)
hOPRK	0, ±15	0, ±45, ±90	0, ±30
hOPRX	0, ±15	0, ±45, ±90	0, ±30, ±120 (H5), 60 (H6), 90 (H6), -60 (H7), -90 (H7)

Table S4. Top 25 structures from fine SuperBiHelix/SuperCombiHelix with mOPRM as the initial template.

Rank	Δθ [°]							Δφ [°]							Δη [°]							E_{CNti} [kcal mol^{-1}]
	H1	H2	H3	H4	H5	H6	H7	H1	H2	H3	H4	H5	H6	H7	H1	H2	H3	H4	H5	H6	H7	
1	0	0	0	0	0	0	0	0	0	0	120	15	-15	0	0	0	0	-30	0	0	0	-352.9
2	0	0	0	0	0	0	0	0	0	0	105	15	-15	0	0	0	0	0	0	0	0	-352.8
3	0	0	0	0	0	0	0	0	0	0	120	15	-15	0	0	0	0	0	0	0	0	-351.3
4	0	0	0	0	0	0	0	0	0	0	105	0	-15	0	0	0	0	-30	0	0	0	-350.7
5	0	0	0	0	0	0	0	0	0	0	75	15	-15	0	0	0	0	-30	0	0	0	-346.9
6	0	0	0	0	0	0	0	0	0	-15	60	30	15	0	0	0	0	0	60	0	0	-345.7
7	0	0	0	0	0	0	0	0	0	0	105	15	0	15	0	0	0	0	0	0	0	-343.7

8	0	0	0	0	0	0	0	0	0	-15	75	15	0	0	0	0	0	0	60	0	0	-342.8
9	0	0	0	0	0	0	0	0	0	0	120	0	0	15	0	0	0	-30	0	0	0	-341.4
10	0	0	0	0	0	0	0	0	0	0	105	0	-15	0	0	0	0	0	0	0	0	-337.5
11	0	0	0	0	0	0	0	0	0	0	90	0	0	15	0	0	0	0	0	0	0	-334.8
12	0	0	0	0	0	0	0	0	0	-15	75	30	15	0	0	0	0	0	60	0	0	-333.8
13	0	0	0	0	0	0	0	0	0	0	90	15	-15	0	0	0	0	0	0	0	0	-333.8
14	0	0	0	0	0	0	0	0	0	0	105	15	-30	0	0	0	0	0	0	0	0	-333.3
15	0	0	0	0	0	0	0	0	0	0	120	15	-30	0	0	0	0	0	0	0	0	-332.7
16	0	0	0	0	0	0	0	0	0	-15	60	-30	15	0	0	0	0	0	30	0	0	-328.9
17	0	0	0	0	0	0	0	0	0	-15	60	-15	0	0	0	0	0	0	0	0	0	-328.1
18	0	0	0	0	0	0	0	0	0	-15	60	-15	15	0	0	0	0	0	0	0	0	-328.1
19	0	0	0	0	0	0	0	0	0	-15	60	-15	0	0	0	0	0	0	30	0	0	-328.0
20	0	0	0	0	0	0	0	0	0	-15	75	-15	0	0	0	0	0	0	0	0	0	-327.8
21	0	0	0	0	0	0	0	0	0	0	120	-15	0	15	0	0	0	-30	0	0	0	-327.6
22	0	0	0	0	0	0	0	0	0	-15	60	30	15	15	0	0	0	0	60	0	0	-327.5
23	0	0	0	0	0	0	0	0	0	-15	75	15	15	0	0	0	0	0	60	0	0	-326.8
24	0	0	0	0	0	0	0	0	0	-15	60	0	0	0	0	0	0	0	0	0	0	-325.9
25	0	0	0	0	0	0	0	0	0	-15	60	-30	0	0	0	0	0	0	0	0	0	-324.3

Table S5. Antagonists' experimental binding constants and their corresponding calculated binding energies relative to M59. The binding energies are calculated according to equation $\Delta G_1 - \Delta G_2 = RT\ln(K_{i2}/K_{i1})$.

Antagonist	K_i [nM]	Relative Binding Energy [kcal mol^{-1}]
M59	3	0.00
M60	23	1.25
M38	113	2.23
M40	524	3.17
M42	>1000	3.57

a)

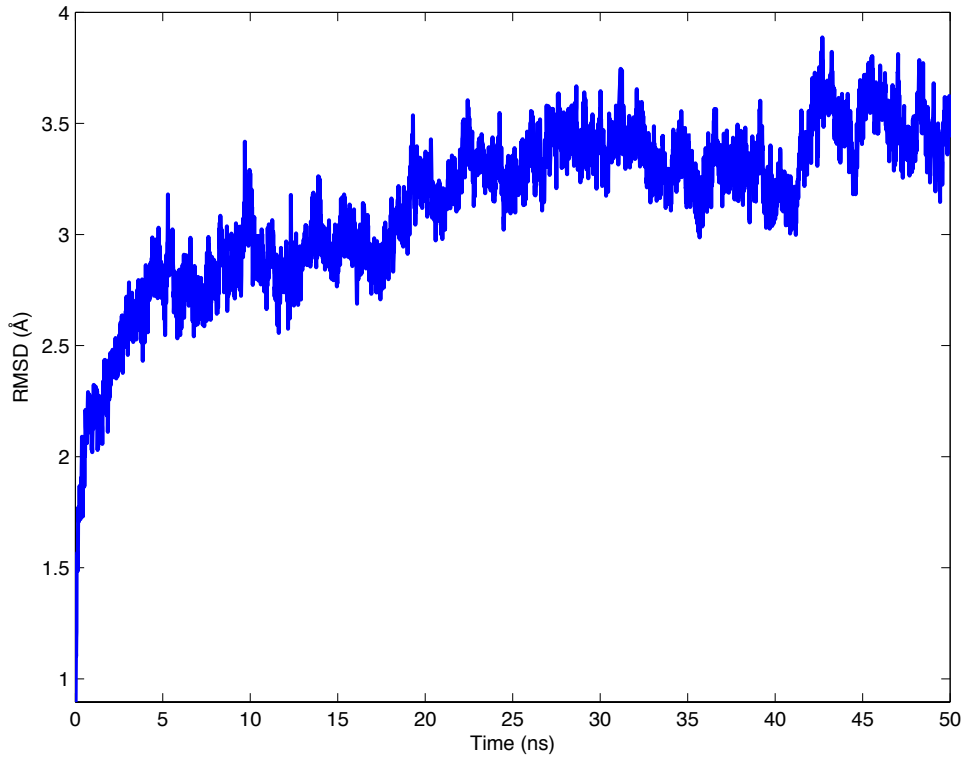

b)

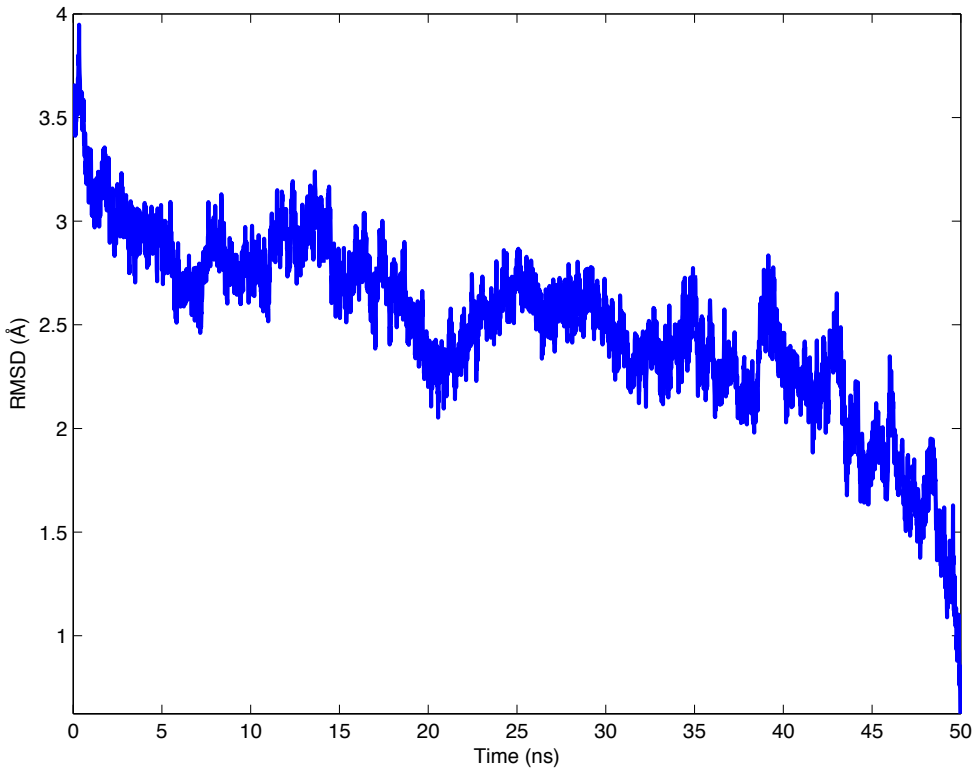

Figure S3. RMSD changes along the MD trajectory. a) The snapshots were aligned against the first frame, and RMSD values were calculated with the first frame as the reference. b) The snapshots were aligned against the last frame, and RMSD values were calculated with the last frame as the reference. Only backbone atoms were considered in calculating RMSD values.

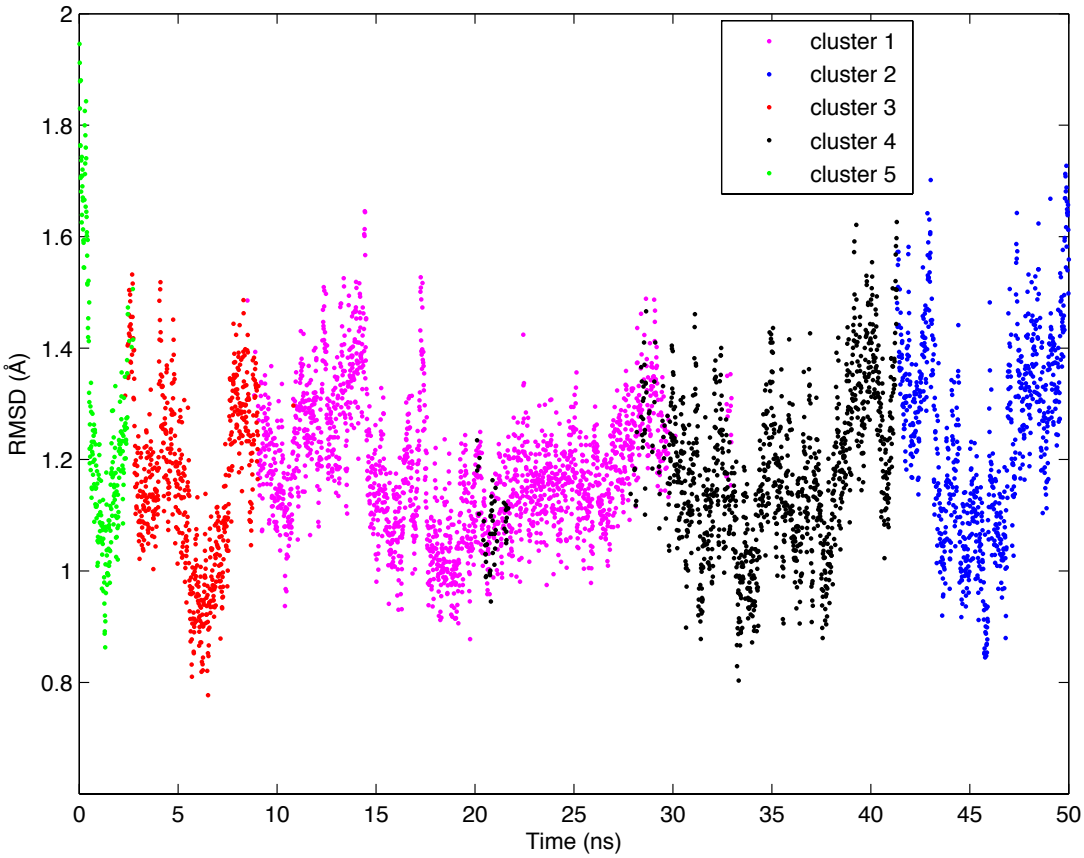

Figure S4. Results of clustering by RMSD along the MD trajectory. K-means algorithm was used. The K-means clustering radius is 2 Å.

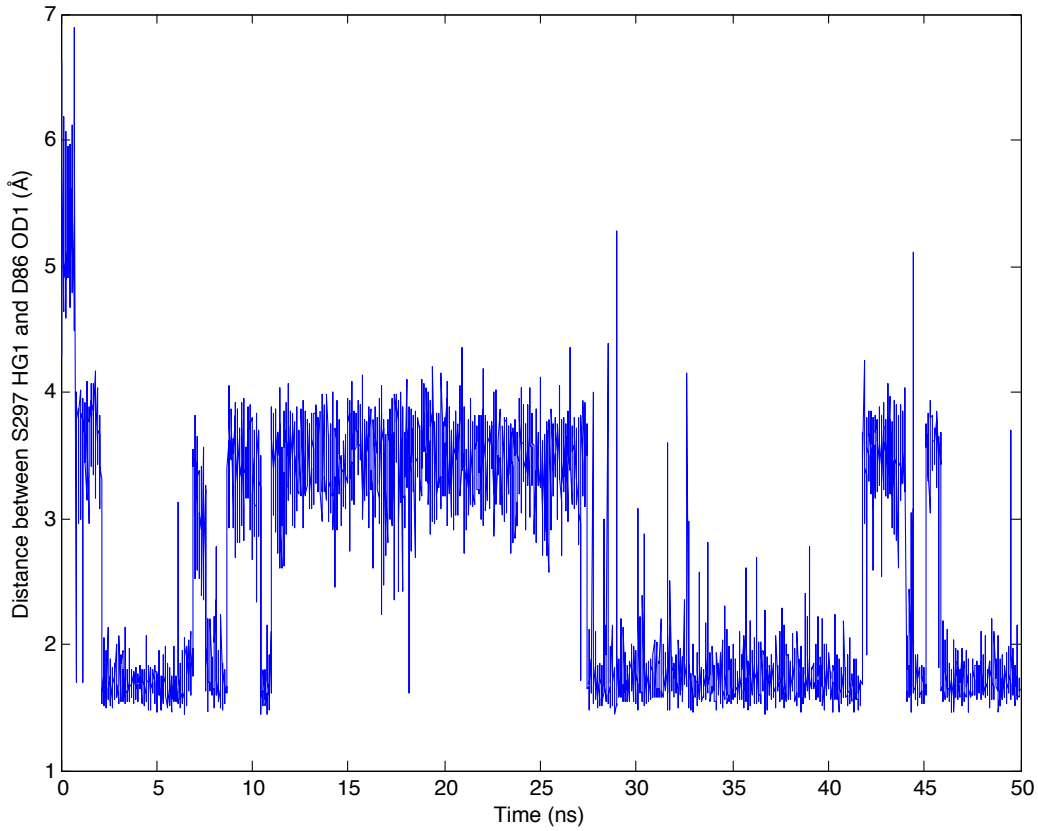

Figure S5. The fluctuation of interatomic distance between S297$^{7.46}$ O-donated H atom and D86$^{2.50}$ O atom on their side chains during the 50 ns MD simulation of M59-bound predicted hSSTR5 structure.

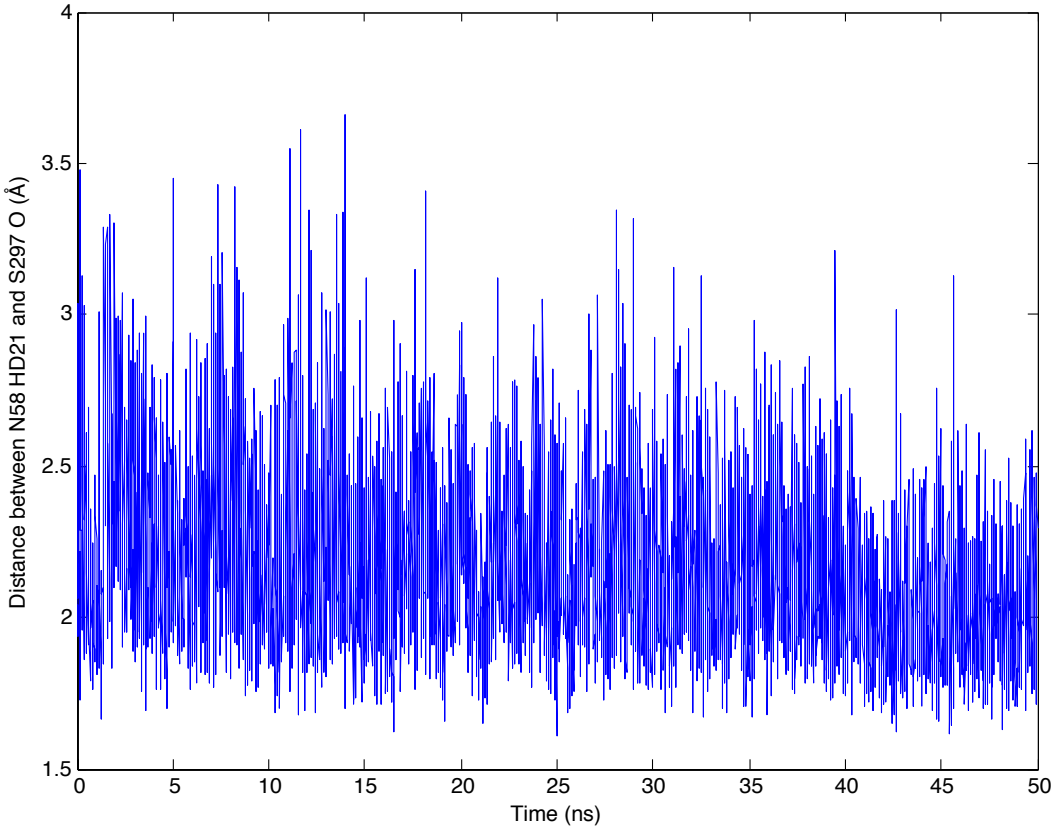

Figure S6. The fluctuation of interatomic distance between N58$^{1.50}$ N-donated H atom on its side chain and S297$^{7.46}$ O atom on its backbone during the 50 ns MD simulation of M59-bound predicted hSSTR5 structure.

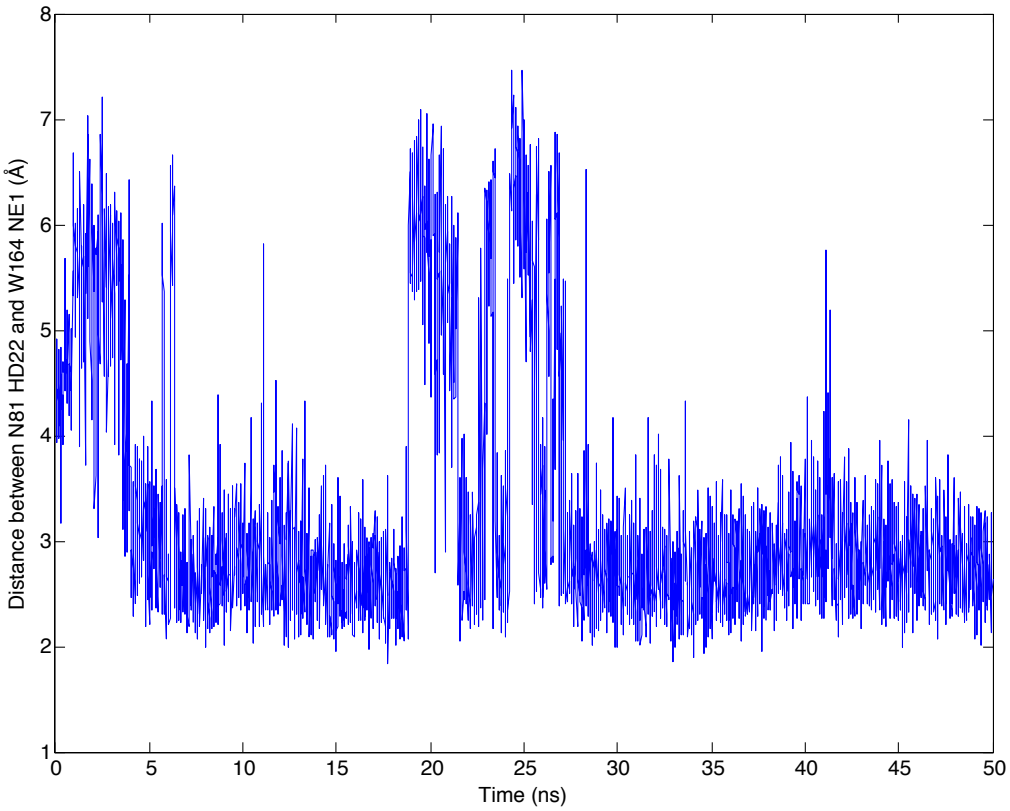

Figure S7. The fluctuation of interatomic distance between N81$^{2.45}$ N-donated H atom and W164$^{4.50}$ N atom on their side chains during the 50 ns MD simulation of M59-bound predicted hSSTR5 structure.

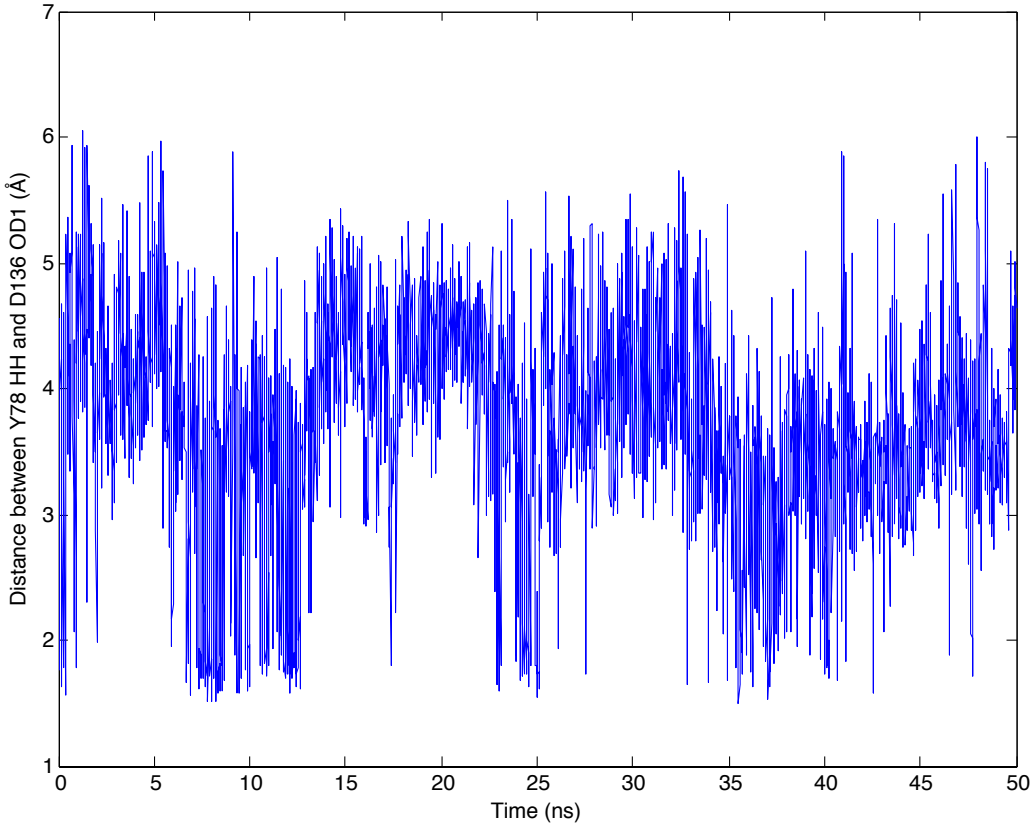

Figure S8. The fluctuation of interatomic distance between Y78$^{2.43}$ O-donated H atom and D136$^{3.49}$ O atom on their side chains during the 50 ns MD simulation of M59-bound predicted hSSTR5 structure.

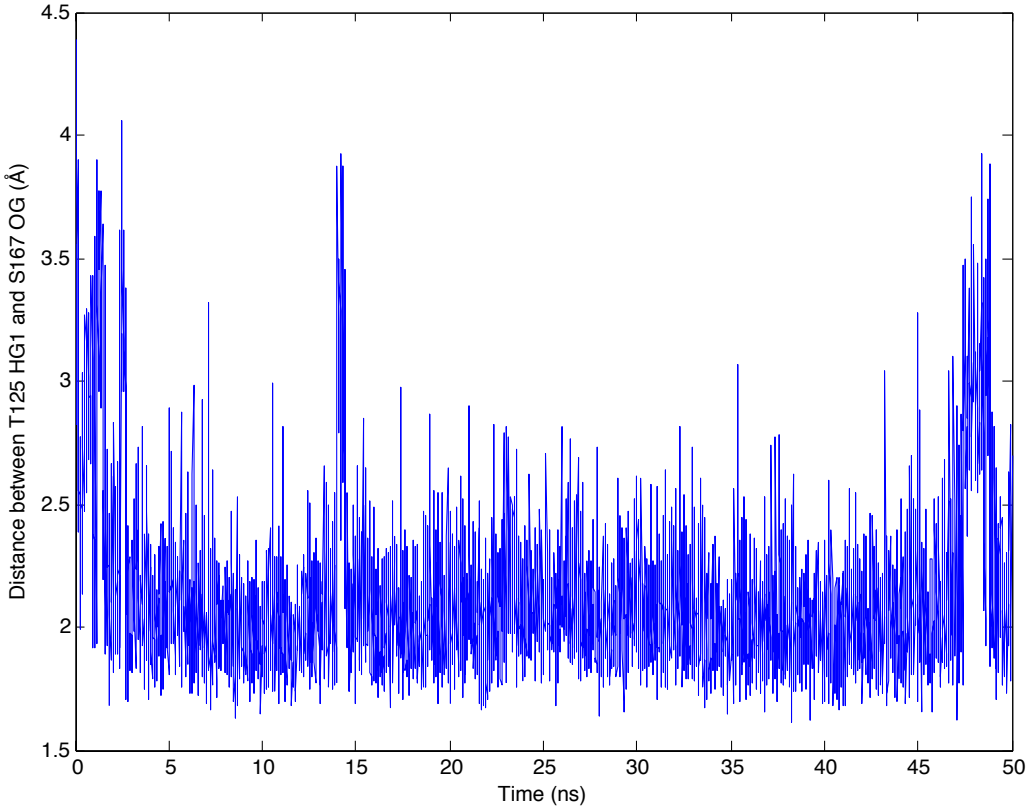

Figure S9. The fluctuation of interatomic distance between T125$^{3.38}$ O-donated H atom and S167$^{4.53}$ O atom on their side chains during the 50 ns MD simulation of M59-bound predicted hSSTR5 structure.

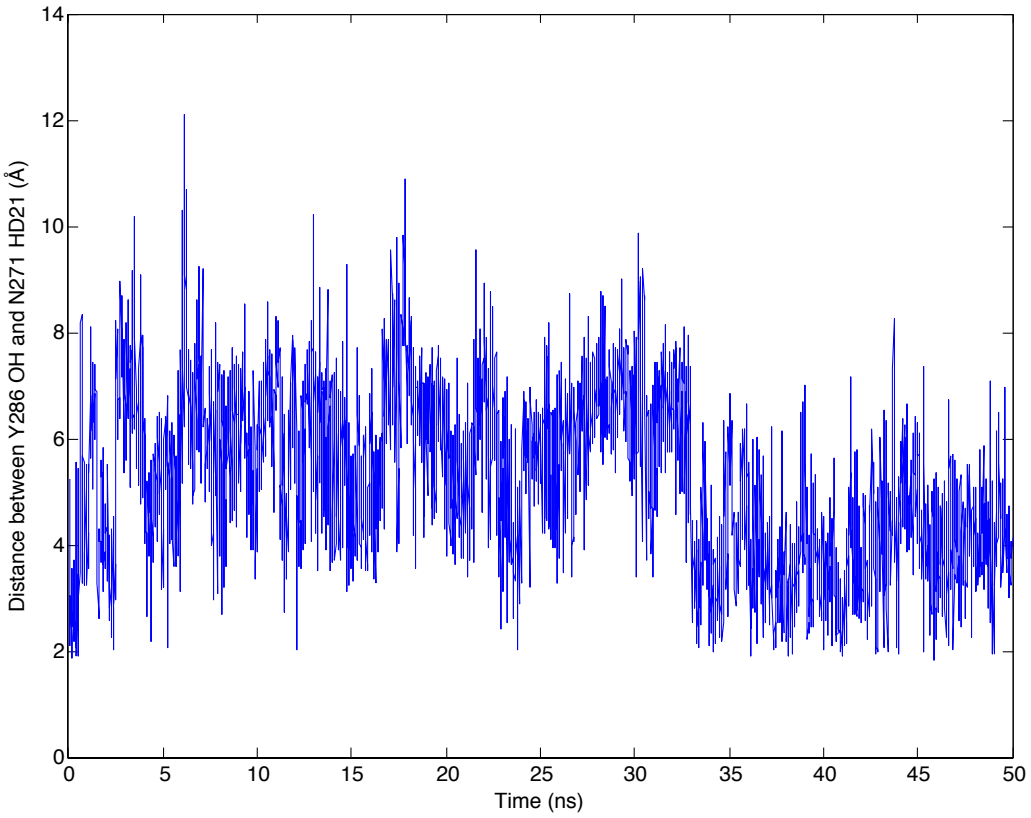

Figure S10. The fluctuation of interatomic distance between N271$^{6.58}$ N-donated H atom and Y286$^{7.35}$ O atom on their side chains during the 50 ns MD simulation of M59-bound predicted hSSTR5 structure.

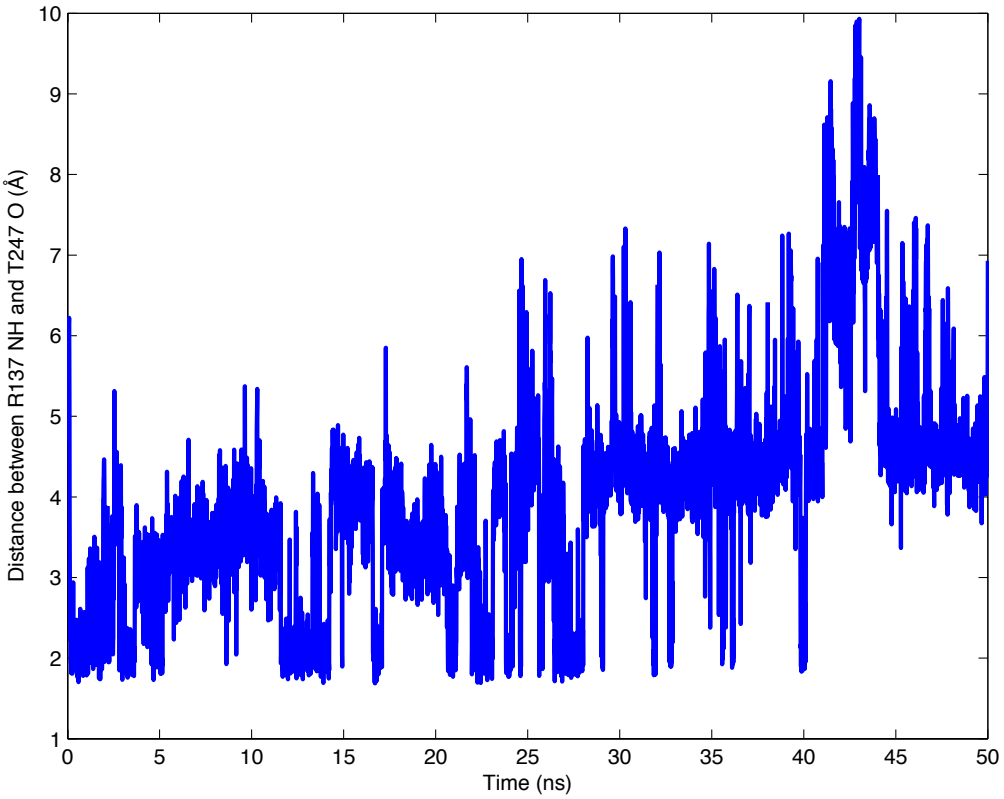

Figure S11. The fluctuation of interatomic distance between R137$^{3.50}$ N-donated H atom and T247$^{6.34}$ O atom on their side chains during the 50 ns MD simulation of M59-bound predicted hSSTR5 structure. Visualization of this interaction is in Figure 7(a) of the main article.

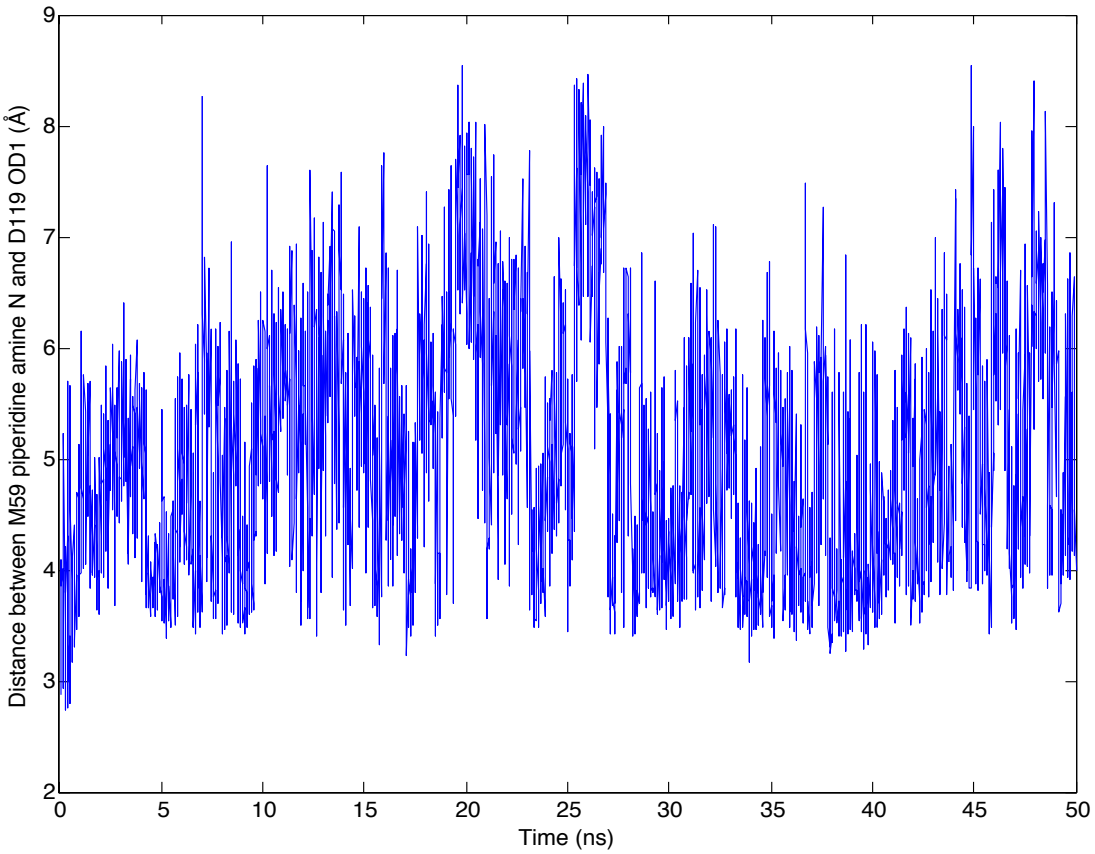

Figure S12. The fluctuation of distance between the M59 piperidine amine N atom and D119$^{3.32}$ carboxylic acid O atom during the 50 ns MD simulation of M59-bound predicted hSSTR5 structure.

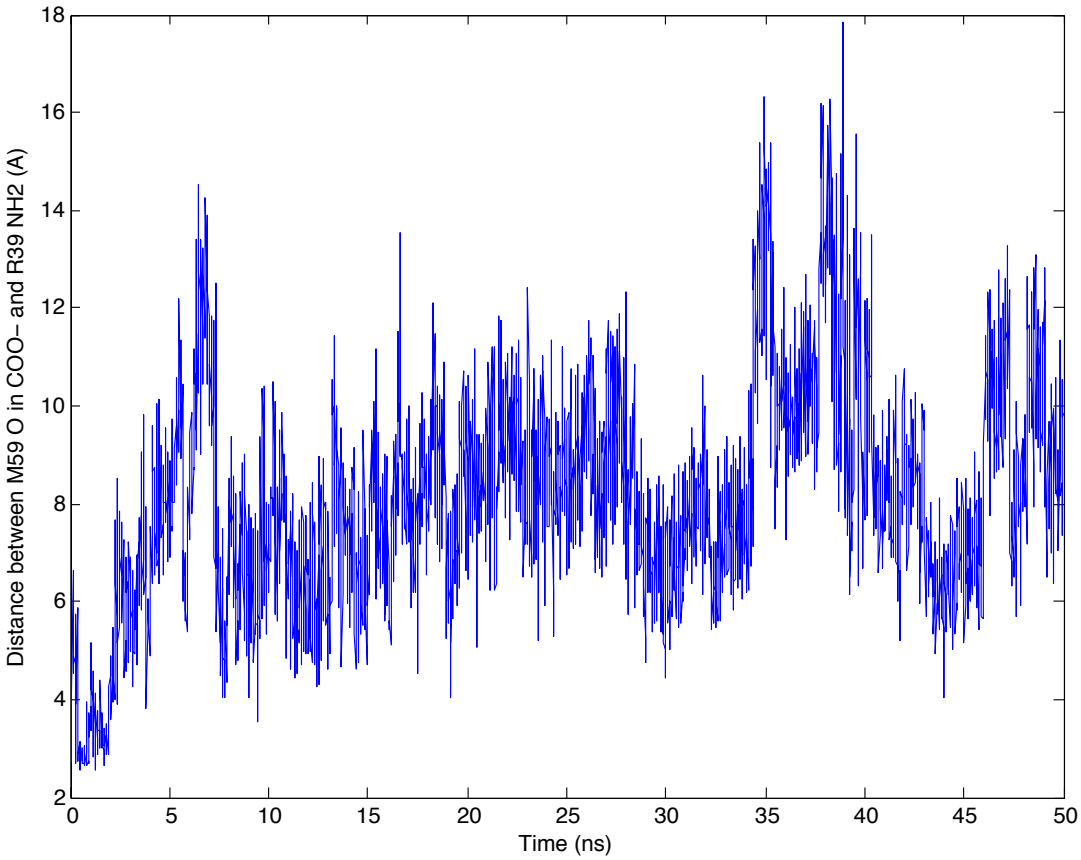

Figure S13. The fluctuation of distance between M59 carboxylic acid O atom and R39$^{1.31}$ amine N atom during the 50 ns MD simulation of M59-bound predicted hSSTR5 structure.

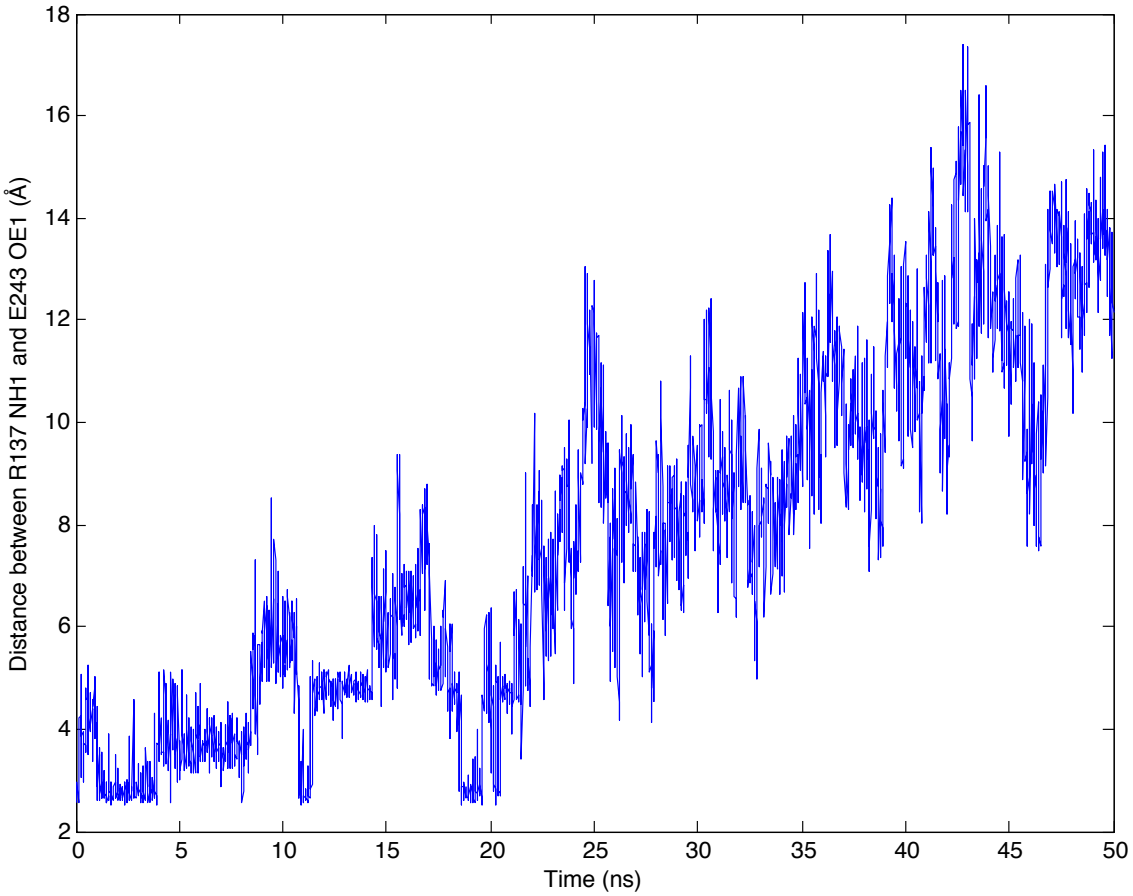

Figure S14. The fluctuation of distance between the R137$^{3.50}$ side chain N atom and E243$^{6.30}$ side chain O atom during the 50 ns MD simulation of M59-bound predicted hSSTR5 structure. After 20 ns, the intracellular end of TM6 including E243$^{6.30}$ unwinds to accommodate the salt bridge between E243$^{6.30}$ and R241 on the loop, and E243$^{6.30}$ can be considered part of the loop.

Additional Experimental Details

1. Preparing the initial helix shape

1.1 OptHelix

This method treats each of the seven helices separately. It first takes the TM lengths predicted above, and generates seven separate canonical polyalanine helices accordingly. Then, it mutates the Pro and Gly back to their respective positions on the helices using Side Chain Rotamer Energy Analysis Method (SCREAM). A first structural optimization is then done to minimize the energy of each helix. Subsequently, the Ser and Thr adjacent to Pro are mutated back, and a molecular dynamics (MD) simulation on each helix is run for 2 ns. Finally, all remaining residues are mutated back to have their original side chains, and a second energy minimization is performed. For each helix, the structures that go to the final step are selected based on "minrmsd", which takes the snapshot that has the average root mean square deviation (RMSD) closest to the average structure from the MD, and based on "mineng", which takes the snapshot that has the lowest energy from the latter 75% of the MD.

1.2 Homology modeling

The template structures were taken from the Orientations of Proteins in Membranes (OPM) database. For each template protein, the sequence was aligned with that of the target protein hSSTR5, and the corresponding residues in the template structure were mutated to be that of the target protein using SCREAM. Then each helix was truncated or extended to the previously determined start/end residues, which

was followed by a geometry optimization of each individual helix for 100 steps using the DREIDING-III force field.[1]

2. Obtaining ActiveConf2

Replacing TM6 shape in the starting structure by that from the active hADRB2 structure: The TMs 1,2,3,4,5,7 of the starting structure and those of the active hβ_2AR x-ray structure were aligned using VMD. Only the backbone atoms were used in the alignment. Then, the TM6 in the starting structure was replaced by that from the active hβ_2AR structure. Finally, the residues on the new TM6 were mutated to hSSTR5 residues using SCREAM.

BiHelix/CombiHelix: After replacing the TM6 shape by that from the active hβ_2AR structure, another BiHelix/CombiHelix step ($\Delta\eta$ from 0° to 360° with a step size of 30°) was carried out before the fine SuperBiHelix. The rest followed BiHelix/CombiHelix described in the main text.

Fine SuperBiHelix sampling: Starting from the best rotation angles from the above BiHelix/CombiHelix, the fine SuperBiHelix/SuperCombiHelix was carried out. The space sampled was: $\Delta\theta$ = 0, ±15°; $\Delta\varphi$ = 0, ±15°, ±30°; $\Delta\eta$ =0, ±30°. The rest followed SuperBiHelix described in the main text.

References

[1] S. L. Mayo, B. D. Olafson, W. A. Goddard, *J. Phys. Chem.* **1990**, *94*, 8897-8909.